Biofilm 3 (2021) 100052

Contents lists available at ScienceDirect

Biofilm

journal homepage: www.sciencedirect.com/journal/biofilm

Competitive advantage of oxygen-tolerant bioanodes of *Geobacter sulfurreducens* in bioelectrochemical systems

Allison M. Speers, Gemma Reguera *

Department of Microbiology and Molecular Genetics, Michigan State University, USA

ARTICLE INFO

Keywords:
Electroactive biofilms
Oxidative stress
Type IV pili
Nanowires
Cytochromes
Transposon mutagenesis

ABSTRACT

Oxidative stress greatly limits current harvesting from anode biofilms in bioelectrochemical systems yet insufficient knowledge of the antioxidant responses of electricigens prevents optimization. Using *Geobacter sulfurreducens* PCA as a model electricigen, we demonstrated enhanced oxygen tolerance and reduced electron losses as the biofilms grew in height on the anode. To investigate the molecular basis of biofilm tolerance, we developed a genetic screening and isolated 11 oxygen-tolerant (oxt) strains from a library of transposon-insertion mutants. The aggregative properties of the oxt mutants promoted biofilm formation and oxygen tolerance. Yet, unlike the wild type, none of the mutants diverted respiratory electrons to oxygen. Most of the oxt mutations inactivated pathways for the detoxification of reactive oxygen species that could have triggered compensatory chronic responses to oxidative stress and inhibit aerobic respiration. One of the mutants (oxt10) also had a growth advantage with Fe(III) oxides and during the colonization of the anode electrode. The enhanced antioxidant response in this mutant reduced the system's start-up and promoted current harvesting from bioanodes even in the presence of oxygen. These results highlight a hitherto unknown role of oxidative stress responses in the stability and performance of current-harvesting biofilms of *G. sulfurreducens* and identify biological and engineering approaches to grow electroactive biofilms with the resilience needed for practical applications.

Introduction

Molecular oxygen (O_2) is often detrimental to the performance of bioelectrochemical systems (BESs), particularly those driven by anaerobic electricigens [9]. The gas readily diffuses through cellular membranes and reacts with enzymes once inside the cells [30], generating Reactive Oxygen Species (ROS) that can cause widespread damage to essential macromolecules (e.g., DNA and proteins) and, eventually, cell death [24,30,65]. Oxygen can be particularly damaging to anode biofilms in microbial fuel cells (MFCs) [45]. Cathode limitations in these BESs often limit the growth of the biofilms on the anode electrode [58]. As a result, oxygen diffuses quickly through the bioanodes and reaches the cells rapidly, diverting respiratory electrons away from the anode electrode and causing substantial drops in power [45]. Depending on the dose and time of exposure, oxygenation can irreversibly damage the biofilm cells and prevent power recovery. This is particularly problematic in MFCs deployed in the field, where oxygen intrusions are quite common [45]. Laboratory MFC prototypes with air-driven cathodes are also prone to power losses due to oxygen crossovers from the cathode to the anode compartment [34]. Increasing the electrode spacing in these systems can minimize interference but this is not always a desirable design [12]. Oxic conditions can also delay the start-up of MFCs and enrich for aerobic bacteria that do not contribute to power generation and/or that compete for electron donors [68]. Facultatively anaerobic electricigens such as those in the genus *Shewanella* can benefit from the presence of oxygen in the anode compartment [63] but the low power densities achieved in these systems limit their applicability [9]. Some enrichment approaches can selectively grow electrically-active anaerobes (mainly *Geobacter*) on the electrode and enrich for aerobic bacteria on top [68]. These stratified systems consume oxygen in the aerobic stratum and prevent the gas from reaching the deeper layers that sustain electricity generation [68]. Yet, the aerobic layer also limits the diffusion of essential nutrients to the electricigenic anaerobes, reducing power density compared to single-layered, anaerobic biofilms [68]. Due to these constraints, researchers typically operate BESs under anoxic conditions [9].

Increasing the oxygen tolerance of anaerobic electricigens could minimize the deleterious impact of oxidative stress on bioanodes and

* Corresponding author. 567 Wilson Rd., Rm. 6190, Biomedical and Physical Sciences bld, Michigan State University, East Lansing, MI, 48824, USA.
E-mail address: reguera@msu.edu (G. Reguera).

https://doi.org/10.1016/j.biofilm.2021.100052
Received 31 March 2021; Received in revised form 18 May 2021; Accepted 19 May 2021
Available online 14 June 2021

improve BES performance. *Geobacter* electricigens are often enriched in mixed-species bioanodes and sustain high power densities in single-species, anoxic BESs [9]. These bacteria are ubiquitous in anaerobic environments where Fe(III) oxides, their natural electron acceptor, and other metals abound [48]. Oxygen intrusions, common in these environments, can promote Fenton-type reactions with the metals and generate cytotoxic hydroxide radicals ($OH^{\bullet}$) [46]. Furthermore, once inside the cell, oxygen can react with enzymes to produce other toxic ROS such as superoxide ($O_2^{\bullet}$) and hydrogen peroxide (H_2O_2) [30]. To overcome toxicity, *Geobacter* genomes encode numerous proteins for ROS detoxification such as catalase, superoxide dismutase and superoxide reductase enzymes [31]. These enzymes prevent ROS accumulation and allow *Geobacter* cells to remain viable after prolonged (up to 24 h in the laboratory) exposure to air [37]. Under microaerophilic conditions, the cells can also use oxygen as an electron acceptor for respiration [37] but higher oxygen concentrations inhibit respiration and cell growth [22]. Transcriptomic analysis in the laboratory representative *Geobacter sulfurreducens* PCA suggests that cells differentially express a cytochrome *bd* menaquinol oxidase to reduce oxygen under microaerobic conditions [22]. As partial oxygen pressure increases, the cells inhibit the terminal oxidase and express capsule genes [22]. Hence, they change the chemistry of the outer surface to protect themselves against oxidative stress, a common antioxidant protection mechanism in bacteria [27]. Genes involved in the biogenesis of *Geobacter* conductive pili are also upregulated with oxygen [22]. The conductivity of the pili allows them to function as protein nanowires [36,49] and provide electronic scaffolds that promote cell-cell aggregation [51] and charge transport in electroactive biofilms [50,60]. Thus, the upregulation of pili by oxygen could trigger adaptive responses (autoaggregation and biofilm formation) that help cells overcome oxygen toxicity.

The concept that *Geobacter* biofilms could provide antioxidant protection is attractive as it could afford opportunities to engineer bioanodes with superior performance in BESs. For example, potentiostatic control of the anode and cathode electrodes in BESs can be used to regulate the growth and the final thickness of electrode-associated biofilms [58]. This, in turn, could modulate the capacity of the electricigenic cells to remain metabolically active and viable after oxygen exposure. The presence in *Geobacter* electricigens of pathways for ROS detoxification could also be harnessed to engineer strains with constitutive and/or enhanced antioxidant protection. Particularly interesting is the ability of some bacteria to secrete a matrix of exopolymeric substances (EPS) to extrude dissolved oxygen [67] and/or scavenge ROS [2,71]. The fact that oxygen toxicity induces the synthesis of a capsule in *G. sulfurreducens* [22] suggests a similar adaptive response for antioxidant protection. This mechanism may also be relevant when growing as biofilms. Indeed, *G. sulfurreducens* biofilms tolerate concentrations of metals that would otherwise kill planktonic cells [15,21], consistent with the activation of pathways to combat metal-induced ROS toxicity [23]. However, little is known about the oxidative stress physiology of *Geobacter* electricigens and how it affects the electroactivity of biofilms. To fill this gap of knowledge, we investigated the oxidative stress response of *G. sulfurreducens* anode biofilms in H-type Microbial Electrolysis Cells (MECs), a BES device that allows for anoxic operation of the anode and cathode compartments and (electro)chemical control of biofilm thickness [58,60]. Using acetate-fed MECs, we demonstrate the increased oxygen tolerance and overall performance of systems driven by thick bioanodes. Furthermore, we screened a library of transposon-insertion mutants and isolated several with enhanced biofilm-forming abilities and antioxidant protection, including one mutant (oxt10) that outperformed the wild type in anoxic and oxic MECs. These results demonstrate that it is possible to improve BES performance by boosting the natural antioxidant responses of bioanodes. Importantly, the study provides novel insights into the oxidative stress physiology of anaerobic electricigens that is critical to engineer strains with the robustness needed for BES applications.

Results and discussion

Effect of anode biofilm thickness on current harvesting in acetate-fed MECs driven by G. sulfurreducens

We grew duplicate MECs of *G. sulfurreducens* under anaerobic conditions with 1 mM or 5 mM acetate, which are conditions that support the growth of thin (~10 μm) or thick (>40 μm) bioanodes, respectively [60]. To test the oxygen tolerance of the biofilms, we introduced 10 ml air into the anode chamber of one of the replicates half-way during the linear phase of current generation, when the biofilms had reached half of their maximum thickness (i.e., ~5 μm or ~20 μm in the 1 mM or 3 mM MECs, respectively) (Fig. 1). The presence of oxygen in the 1 mM acetate MEC led to a rapid drop in current, as cells diverted respiratory electrons towards the detoxification of ROS and/or respiration of oxygen (Fig. 1). By contrast, MECs fed with 5 mM acetate only experienced some minor losses in power (Fig. 1). We calculated that oxygen intrusion in the 1 mM acetate MECs had led to the loss of 58% of the electrons harvested as electrical currents in the anoxic controls. By contrast, the thicker biofilms exposed to oxygen in the 5 mM acetate MECs only lost 8% of the electrons recovered in the anoxic controls. The increased oxygen tolerance of the bioanodes cannot merely be the result of constraints to passive gas diffusion through the thicker biofilms, because acetate, which has a much lower diffusion coefficient than oxygen in biofilms [61], is not diffusion-limited in MEC bioanodes as thick as 200 μm when provided in similar concentrations [4]. Furthermore, oxygen can passively diffuse through even thicker biofilms (up to 1–2 mm) [44]. The most likely explanation is that the biofilm cells reprogrammed their physiology as they grew in multilayered communities, activating biofilm-specific mechanisms for oxidative stress resistance [29,42]. These mechanisms may have included chemical changes to the EPS matrix for improved ROS detoxification but also oxygen extrusion. The latter could have allowed the thick biofilms to prevent the permeation of oxygen and its use as an electron acceptor for respiration, thereby minimizing electron losses in the 5 mM MECs (Fig. 1).

Isolation of oxygen-tolerant (oxt) mutants with enhanced biofilm formation

Growth within colonies can often reproduce many of the physiological states of cells living within biofilms [43]. Thus, we developed a genetic screening to identify transposon-insertion mutants that could grow as colonies in the presence of oxygen (Fig. 2A). For this experiment, we mixed aliquots of a transposon-insertion library of

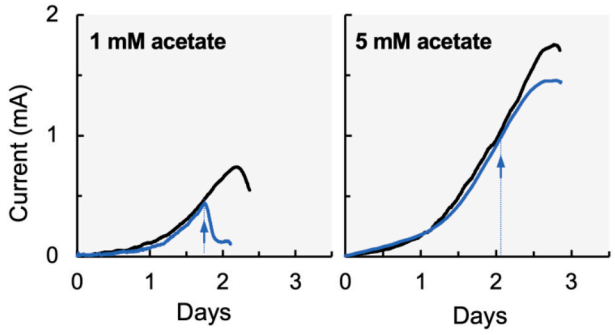

Fig. 1. Effect of oxygen exposure on current generation in MECs fed 1 mM or 5 mM acetate. We grew duplicate MECs with 1 mM or 5 mM acetate to grow thin (~10 μm) or thick (~40 μm) biofilms on the anode electrode and introduced air (10 ml) in one of them (arrow) mid-way during the linear phase of current generation. Current production in the anoxic MEC controls is shown in black and in the oxygenated MECs, in blue. (For interpretation of the references to color in this figure legend, the reader is referred to the Web version of this article.)

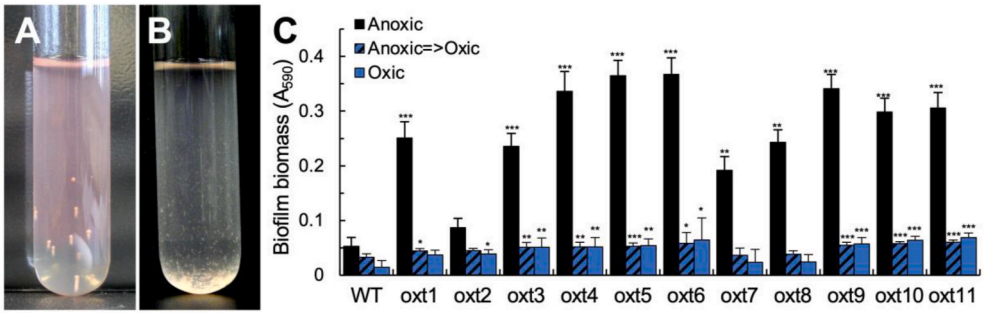

Fig. 2. Isolation and aggregative phenotypes of oxt mutants. (A–B) We isolated 11 oxt mutant colonies that grew in the top regions of soft agar tubes (highest oxygenation, as indicated by the pink color of oxidized resazurin) **(A)** and flocculated extensively when grown in FWAF broth at 30 °C for 48 h **(B). (C)** The oxt mutants had enhanced biofilm-forming abilities (measured with the crystal violet dye at 590 nm) when grown anaerobically (solid black) and, in many cases, when exposed to air after 30 h of incubation (blue stripes) or throughout the incubation period (solid blue). Shown are average and standard deviation of 5 replicates per strain per condition. The asterisks show significant differences between the oxt mutants and wild type (WT) in two-tailed t-tests for each culture condition (*, $p < 0.05$; **, $p < 0.005$; ***, $p < 0.0005$). (For interpretation of the references to color in this figure legend, the reader is referred to the Web version of this article.)

G. sulfurreducens with anoxic NBAFYE medium solidified with 0.3% Noble agar and added resazurin as a redox indicator. After a short incubation in the soft-agar tubes to enrich for mutants without growth defects, we sparged the headspace of the tubes with filter-sterilized air to establish an oxygen gradient (pink color) along the top ¾ of the soft-agar culture and incubated the tubes at 30 °C to enrich for oxygen-tolerant mutants (Fig. 2A). We recovered from the top layer of the tubes (highest oxygenation) 11 colonies, which we designated as oxygen-tolerant mutants (oxt) 1 to 11. All of the mutants grew planktonically under anaerobic conditions once transferred to anoxic FWAF medium though they flocculated and attached to the tube's walls substantially (Fig. 2B). This aggregative behavior is typical of mutants with activated oxidative stress responses [18,39]. Furthermore, all but one (oxt2) of the mutants formed denser biofilms under anaerobic conditions and some were also able to accumulate more biofilm biomass when air was introduced after the first 30 h of anaerobic incubation or was present from the beginning (Fig. 2C). Such aggregative behaviors are again consistent with mutations that activate or even exacerbate oxidative stress responses.

Sequencing of the transposon's flanking regions in each oxt mutant identified the genomic insertion of the Tn*5* in different genes, including some that are predicted to be involved in oxidative stress responses (Table 1). For example, the oxt1 mutant carried the Tn*5* transposon in the A subunit (GSU0466) of one of two cytochrome *c551* peroxidases (Ccp-1) encoded in the genome of *G. sulfurreducens* [52]. This protein was first described as a diheme cytochrome of the electron transport chain that reduces Fe(III) citrate in the cell's periplasm and was accordingly named the '*metal-reduction-associated cytochrome*' MacA [10]. The protein was later shown to have peroxidase activity and to play roles in the periplasmic detoxification of ROS [52]. The inactivation of MacA in the oxt1 mutant could increase ROS-induced stress in the periplasm and trigger a generalized transcriptional response against oxidative stress. Oxt2, on the other hand, carried the Tn*5* insertion in the glutamyl-tRNA reductase (GSU3284, HemA) that catalyzes the first committed step in heme biosynthesis [19]. Bacteria tightly regulate *hemA* expression to modulate heme biosynthesis under anaerobic (high levels) and aerobic (low levels) conditions [20]. The inactivation of *hemA* in the oxt2 mutant is expected to reduce heme biosynthesis and, by extent, heme-induced accumulation of ROS [3]. Thus, this mutant may have low levels of endogenous ROS production. This could explain why oxt2 was the only mutant that did not aggregate substantially and only formed dense biofilms after prolonged exposure to air (Fig. 2C).

Oxt3 is inactivated in a gene (GSU2093) that codes for the ATP-binding protein of an ABC (ATP-binding cassette) superfamily transporter. These membrane-bound transporters mediate the uptake and extrusion of many different substrates such as ions and small (e.g., amino acids, sugars, xenobiotics, and vitamins) or large (e.g., peptides and polysaccharides) molecules [41]. A search of the genome region around GSU2093 failed to identify additional ABC subunits, consistent with the monomeric organization of extrusion transporters [41]. The only gene annotated in this region is an NADH oxidase (GSU2095) that could couple the reduction of oxygen or peroxide (H_2O_2) to the oxidation of NAD(P)H to $NAD(P)^+$ and recycle the NAD^+ cofactor. Future work should consider whether polar effects of the Tn*5* insertion in the GSU2093 transporter could have indirectly affect the transcription of the NADH oxidase and the oxidative stress response. Oxt4, on the other hand, represents a mutation that could lead, at least indirectly, to the compensatory activation of stress response pathways. The Tn*5* insertion in the oxt4 mutant (GSU1572) inactivated a homolog of the dihydrofolate reductase enzymes that catalyze the NADPH-dependent conversion of dihydrofolate to tetrahydrofolate. The latter is a precursor of thymidylate and purine nucleotide biosynthesis that, at least in eukaryotes, is responsive to redox stress [38]. Mutations in bacterial dihydrofolate reductase enzymes can lead to the emergence of antimicrobial resistance phenotypes [1], consistent with a pleiotropic effect of the oxt4 mutation in the activation of stress response pathways.

Oxt 5 carried the Tn*5* in a hypothetical gene (GSU0710) within a largely uncharacterized genomic region, preventing functional predictions. By contrast, Oxt6 (GSU3173) was inactivated in the needle sheath protein TssC of a type VI secretion system (T6SS). Although T6SS are typically recognized as contact-dependent machineries for protein translocation, they can also mediate contact-independent functions critical to manganese uptake and oxidative stress survival [54]. These functions are under the control of OxyR, the master regulator of the bacterial stress response [54]. The inactivation of the T6SS of *G. sulfurreducens* is thus expected to disrupt metal homeostasis and trigger compensatory mechanisms for antioxidant protection. Oxt7, on the other hand, was inactivated in OmcO (GSU2912), an outer membrane *c*-type cytochrome cytochrome that is needed for the growth of thick biofilms [14]. The fact that OmcO is needed to grow thick biofilms and that these biofilms have increased oxygen tolerance suggest roles for this cytochrome in antioxidant protection. Its inactivation in the oxt7 mutant may have triggered compensatory effects in other oxidative stress pathways, as we hypothesized for other mutants.

Supporting the notion that transcriptional reprogramming is needed

Table 1
Genetic identification of oxygen tolerant (oxt) mutants.

Strain	Locus tag	Gene annotation
oxt1	GSU0466	Cytochrome c551 peroxidase CcpA-1 (MacA)
oxt2	GSU3284	Glutamyl-tRNA reductase (HemA)
oxt3	GSU2093	ABC transporter, ATP-binding protein
oxt4	GSU1572	RibD domain-containing protein
oxt5	GSU0710	Hypothetical protein
oxt6	GSU3173	Type VI secretion system needle sheath protein (TssC)
oxt7	GSU2912	Cytochrome c family protein (OmcO)
oxt8	GSU2224	Response regulator
oxt9	GSU0376	Glycine cleavage system H protein (GcvH-1)
oxt10	GSU1725	Nuclease SbcCD, C subunit, putative
oxt11	GSU3289	Conserved hypothetical protein

for oxygen tolerance, oxt8 was inactivated in a cytosolic Asp-phosphoresponse regulator (GSU2224). The gene is flanked by chemotaxis sensory proteins (GSU2222, CheA; GSU2223, CheY-6) and two GTP-binding proteins, including one (EngA, GSU2225) that is homologous to an *E. coli* protein implicated in ribosome stability and/or biogenesis [8]. The presence of a histidine kinase sensor (CheA) upstream of the GSU2224 regulator suggests that both CheA and the GSU2224 regulator could work coordinately to transduce a chemotaxis response in *G. sulfurreducens*. Given the cytotoxicity of oxygen above microaerobic concentrations, cells are likely to activate avoidance responses [53]. Inactivation of the response regulator could impair the flight or fight chemotactic response and trigger alternative stress-related responses such as the expression of an extracellular polysaccharide needed for cell-cell aggregation and biofilm formation.

Oxt9 carries the Tn*5* insertion in GSU0376, which codes for one (H protein) of the four proteins of the glycine cleavage pathway. This tetrameric complex catalyzes the reversible oxidation of glycine to serine using NAD^+ as cofactor, thereby regulating glycine levels and controlling glutathione production and other defense pathways against oxidative stress [32]. Its inactivation in the oxt9 mutant could lead to the accumulation of glycine, stimulating protein synthesis and reducing oxidative stress [66]. Similarly, the oxt10 mutant is inactivated in a protein (subunit C of the SbcCD nuclease) that repairs ROS-induced damage and could indirectly activate compensatory pathways to increase ROS tolerance. In *E. coli*, SbcCD cleaves hairpin structures that halt the progress of replication forks [16]. The single-stranded endonuclease activity of the complex can also blunt dsDNA breaks to facilitate recognition and repair by the RecBCD complex [69]. This allows the homologous recombination machinery of the cell to restore damaged and/or collapsed replication forks and resume DNA replication. Replication stress is common during the cell cycle even in the absence of external stressors [70]. Without SbcCD, cells accumulate DNA damage and induce the SOS response, activating repair pathways commonly associated with cellular responses to external stressors [62]. Indeed, inactivation of *sbcC* and other repair proteins can constitutively induce and/or overexpress protective pathways and lead to a chronic state of oxidative stress that reduces genotoxicity [65]. Compensatory effects are also expected from the inactivation of the DNA condensation functions of SbcCD. As a member of the SMC (structural maintenance of chromosomes) family, the complex is predicted to play roles in DNA folding [55]. By affecting genome condensation, SbcCD could influence the transcription of many genes in the genome and the widespread reprogramming of cellular functions. In support of this, mutations in *sbcCD* in *Acinetobacter baylyi* substantially increase foreign DNA acquisition during natural transformation [28].

The last oxt mutant recovered from the soft-agar tubes (oxt11) was inactivated in a conserved hypothetical protein (GSU3289) containing a rubrerythrin domain (Pfam PF02915). Rubrerythins are non-heme diiron proteins of the ferritin-like superfamily that scavenge peroxide in many organisms [11]. The absence of a C-terminal rubredoxin-like domain in GSU3289 rules out electron transport functions and suggests relatedness to the rubrerythin peroxidases that evolved as part of the adaptation of some anaerobic archaeal and bacterial lineages to microaerophilic environments [11]. Consistent with this, GSU3289 clusters in the genome with the peroxide stress regulator PerR (GSU3292) and another rubrerythin (GSU3293). Thus, almost all of the oxt mutants carry inactivating mutations in pathways needed for antioxidant protection. Given the aggregative nature and enhanced biofilm-forming abilities of these mutants (Fig. 2), the oxt mutations may have triggered widespread responses for antioxidant protection, including the upregulation of capsule genes needed to protect the cells against otherwise lethal concentrations of oxygen [22].

The oxt mutants tolerate but cannot respire oxygen

The WT strain of *G. sulfurreducens* can survive exposure to air for up to 24 h and can grow with oxygen as electron acceptor under microaerobic (~10% v/v oxygen) conditions [35]. We performed similar experiments to test the ability of the oxt mutants to tolerate (Fig. 3A) and respire (Fig. 3B) oxygen in reference to the WT controls. We first tested the oxygen tolerance of the strains by growing the cells in a MOPS-buffered medium at 35 °C for 36 h in the presence or absence of oxygen and then comparing their recovery under anaerobic conditions (Fig. 3A). All of the strains resumed growth after being exposed to air for 36 h, sustaining growth rates ($5.9 \pm 0.4\ d^{-1}$) similar to those in the anaerobic controls ($5.9 \pm 0.2\ d^{-1}$). Despite growing at similar rates, the WT cultures reached a higher OD_{600} (1.23 ± 0.02) than the oxt strains (1.02 ± 0.03) (Fig. 3A). We hypothesized that oxygen carried over with the inoculum could have supported respiratory growth and boosted growth yields in the WT but not in the mutants. To test this, we investigated the ability of the WT and oxt mutants to grow with oxygen as the sole electron acceptor (Fig. 3B). For this experiment, we grew all of the strains anaerobically in the same MOPS-buffered medium with acetate as electron donor (20 mM) but reduced the amount of fumarate (20 mM instead of 40 mM) to arrest cell growth as soon as the electron acceptor was depleted (~36 h). At this time, all of the strains had reached a similar OD_{600} (0.53 ± 0.03). We then introduced air in the headspace to provide oxygen (10% v/v) as an electron acceptor for acetate-dependent growth. While the WT cells resumed growth rapidly after introducing air (as indicated by the increases in OD_{600} to 0.68 ± 0.01), the oxt mutants remained in stationary phase (Fig. 3B). The inability of the oxt mutants to respire oxygen could reflect their inability to express the terminal oxidases of the aerobic respiratory pathway. Alternatively, the mutants may have acquired mechanisms to prevent the permeation of oxygen inside the cells, as reported for bacteria that produce oxygen-extruding biopolymers [67].

Competitive advantage of the oxt10 mutant during the reduction of Fe(III) oxides and anode electrodes in MECs

As in current-harvesting biofilms [50,60], *G. sulfurreducens* also expresses conductive pili to grow with Fe(III) oxides [49]. The conductive pilus fibers function as nanowires between the cell and the extracellular mineral particles, discharging respiratory electrons at rates that greatly exceed the rates of cellular respiration [36]. By reducing the oxides at a distance from the cell surface, the pili also minimize metal-induced oxidative stress [67]. Thus, we investigated the ability of the oxt mutants to grow by coupling the oxidation of acetate to the reduction of Fe (III) oxides. For these experiments, we first grew the strains in a medium with acetate and poorly crystalline Fe(III) oxides that contained low levels (1 mM) of the metal chelator nitrilotriacetic acid (NTA) to alleviate the need for cells to contact the minerals and stimulate growth [59]. We then transferred the cells to Fe(III) oxide media without NTA and evaluated the growth of the mutants in reference to WT controls. All of the oxt mutants had severe (oxt2, oxt5, oxt7 and oxt11) or mild (oxt1, oxt3, oxt4, oxt6, oxt8 and oxt9) growth defects, except for oxt10, which grew faster than the WT. A second transfer in Fe(III) oxide media without NTA aggravated the growth defects of the oxt1-9 and oxt11 mutants and reproduced the growth advantage of the oxt10 mutant compared to the WT (Fig. 3C). High concentrations of metal nanoparticles, as in the Fe(III) oxide cultures, cause oxidative stress and cytotoxicity [25]. As a result, WT cells typically undergo a phase of acclimation in the Fe(III) oxide cultures that shows as a *lag* phase (~6 days before Fe(II) is detected) (Fig. 3C). Yet, the oxt10 mutant did not require acclimation and resumed exponential growth with the Fe(III) oxides without delay. Furthermore, although the solubilization of Fe(II) from the Fe(III) oxides can disrupt redox homeostasis and generate ROS [26], the oxt10 cells doubled more rapidly (6.5 ± 1.0 days) than the WT cells (9.1 ± 0.9 days) ($p = 0.028$). Thus, increased antioxidant protection in the oxt10 mutant confers on the cells a growth advantage during the reduction of Fe(III) oxides.

Oxidative stress can also delay the colonization of the anode

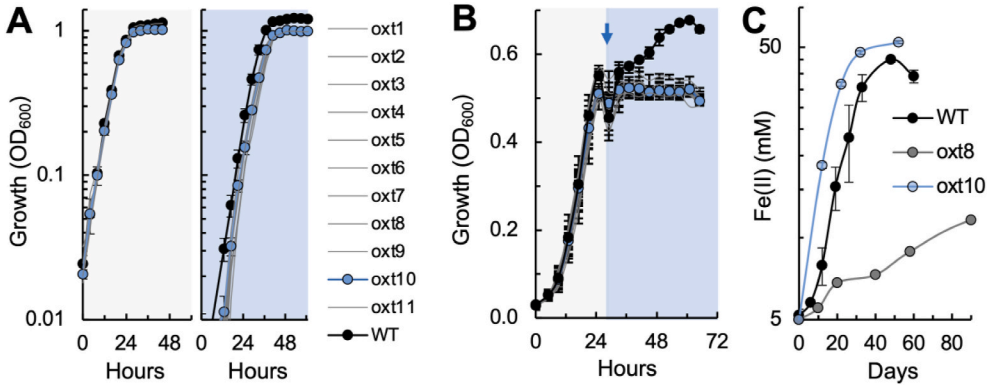

Fig. 3. Growth of WT and oxt mutants with fumarate in the presence or absence of oxygen (A–B) and with Fe(III) oxides (C). (A) Growth in anaerobic MOPS-buffered NBAFYE medium (20 mM acetate and 40 mM fumarate) at 35 °C of WT (black) or oxt (gray, except oxt10 in blue) strains. The cultures were started with cells previously grown anoxically (gray) or in the presence of air (blue) for 36 h. The similar recovery of the WT and oxt mutants after oxygen exposure suggests similar levels of oxygen tolerance. **(B)** Growth of the WT and oxt mutants at 35 °C in anoxic NBAFYE-MOPS without cysteine and with growth-limiting concentrations of fumarate (20 mM) (gray area). The strains grew at similar rates and entered stationary phase as soon as they depleted fumarate (~36 h). Introducing air (10% v/v oxygen, blue area) in the culture's headspace (arrow) supported oxygen-dependent growth in the WT but not in the oxt mutants. **(C)** Growth of the WT and oxt mutants (oxt8, gray; oxt10, blue) that grew in FW medium with acetate and Fe(III) oxides (125 mM) at 30 °C (measured as the amount of acid-extractable Fe(II) with the ferrozine assay). (For interpretation of the references to color in this figure legend, the reader is referred to the Web version of this article.)

electrode in MECs. To test this, we compared the performance of the WT and oxt10 mutant in acetate-fed (1 mM and 3 mM) MECs (Fig. 4). As in the Fe(III) oxide cultures, the oxt10 generated current faster than the WT (Fig. 4A). The rapid start-up allowed the oxt10 mutant to reach 0.3 mA of current by the time the WT MECs started the linear phase of current acceleration (~24 h post-inoculation). The oxt10 advantage was clearly during the colonization of the electrode because, once attached, both the mutant and WT cells generated current at similar rates (0.051 ± 0.003 mA/h in duplicate MECs) (Fig. 4B). Charge transfer resistance is high [7] and frequency shifts are common during the initial attachment phase (~15 h) that precedes the formation of WT electroactive biofilms [6]. These shifts in frequency are similar to those caused when biopolymers adhere to an electrode surface [6]. This is consistent with the expression by WT cells of surface polymers (e.g., capsule, EPS layer, etc.) to irreversibly attach to the electrode and begin its reduction. Further supporting this, an unbiased genetic screen identified colonization-defective mutants of *G. sulfurreducens* that carried inactivating mutations in genes encoding proteins for the synthesis and modification of extracellular polymers (capsule, lipopolysaccharide and exopolysaccharide) [14]. The constitutive expression of a polymeric matrix by the oxt10 mutant could promote adhesion to the electrode surface, minimizing unproductive interactions and promoting rapid colonization. This very same polymeric matrix could provide a protective mechanism against oxidative stress, as reported for other bacteria [47,64]. Extracellular polysaccharides, for example, can facilitate attachment to surfaces and also detoxify ROS [2,71]. Furthermore, some EPS layers can effectively extrude dissolved oxygen [67], providing a plausible explanation for the inability of the oxt10 mutant to grow in the presence of oxygen (Fig. 3B). This is of particular importance in MECs,

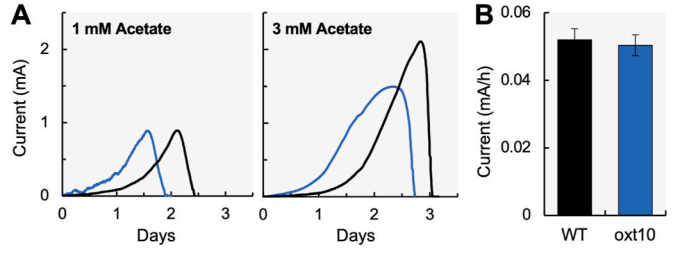

Fig. 4. MEC performance of oxt10 mutant compared to WT. (A) Representative plots of current generation in WT (black) and oxt10 (blue) MECs fed with 1 mM or 3 mM acetate. **(B)** Average rate of current production for the WT and oxt10 mutant in duplicate MECs. (For interpretation of the references to color in this figure legend, the reader is referred to the Web version of this article.)

where oxygen intrusions can divert a significant fraction of respiratory electrons from the anode biofilms.

Rapid recovery of oxt10 anode biofilms after oxygen intrusions in MECs

The results presented thus far suggest that the surface chemistry of the oxt10 mutant is well suited for antioxidant protection and oxygen extrusion. To test this, we grew thin (~ 5 μm) biofilms of the oxt10 and WT strains on the anode electrode of MECs fed with 1 mM acetate before introducing oxygen into the anode chamber (Fig. 5A). As we showed previously (Fig. 1), the oxygen intrusion caused a rapid drop in current upon oxygenation of the WT MECs because the biofilms are too thin to provide antioxidant protection (Fig. 5A). The oxt10 MECs also experienced drops in current production after oxygenation (Fig. 5A), but at rates 1.5-fold lower than the WT (p = 0.03) (Fig. 5B). Furthermore, current production in the oxt10 MECs resumed rapidly after restoring anoxic conditions in the anode chamber (Fig. 5A) and did so at rates more than two-fold higher than those recorded during the anoxic recovery of the WT MECs (Fig. 5B). Recovery in the WT MECs was also delayed for 4–5 h (Fig. 5A). During this time, the WT planktonic cells aggregated and attached to the glass walls of the anode chamber, an adaptive response of bacterial cells to oxidative stress [39]. Thus, oxygen toxicity was high in the WT MECs and, as a result, electricigenic recovery was delayed. By contrast, the anode chamber in the oxt10 MECs remained turbid after oxygenation, as expected of a mutant that is constitutively activated for antioxidant protection. Such chronic response to oxidative stress protected the planktonic and biofilm cells from oxidative damage during the oxygen intrusion, allowing the bioanodes to restore current production without delay (Fig. 5A) and at faster rates than those measured during the anoxic recovery of the WT bioanodes (Fig. 5B).

We also investigated if growing thicker oxt10 biofilms could improve MEC performance in the presence of oxygen (Fig. 5C). For these experiments, we grew oxt10 biofilms in 1 mM acetate MECs until all the electron donor had been oxidized and current production had reached baseline levels. We then replenished acetate in the anode chamber and introduced oxygen (10 ml of air; blue area in Fig. 5C). Current harvesting was immediately restored in the MECs despite the presence of oxygen. Furthermore, the bioanodes remained viable throughout the oxygenation phase because they continued to grow on the electrode and to harvest current once anoxic conditions resumed and acetate was provided as electron donor (Fig. 5C). These results show that it is possible to boost the natural antioxidant defenses of *G. sulfurreducens* via genetic engineering and by operating the MECs under conditions that

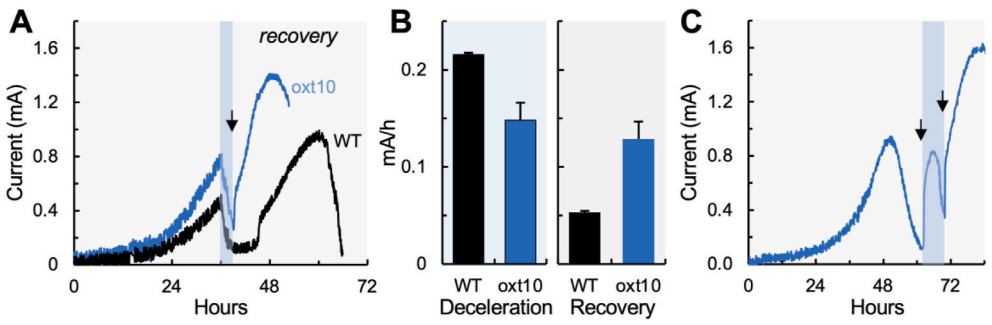

Fig. 5. Oxygen tolerance of the oxt10 mutant in MECs fed with 1 mM acetate. (A) Drop and recovery of current harvesting after the introduction of air (20 ml or 168.6 μmol oxygen; blue area) in the anode chamber of WT (black) and oxt10 (blue) MECs during the linear phase of current generation. Once the current dropped to baseline levels, we sparged the anode compartment with oxygen-free N_2:CO_2 to restore anoxic conditions and added acetate (0.5 mM; arrow) while monitoring the recovery of current production by the bioanodes. **(B)** Average deceleration rates in duplicate WT and oxt10 MECs during oxygen exposure (blue area in (**A**)) mutant and average rates of electrical current recovery after anoxic conditions resume (gray recovery area in (**A**). **(C)** Oxt10 bioanodes grown with acetate (1 mM) under anoxic conditions resume current harvesting in the presence of oxygen (84 μmoles or 10 ml of air; blue area) after the addition of acetate (0.5 mM, first arrow). The bioanodes continue to grow and produce current under anoxic conditions after acetate refeeding (5 mM, second arrow). (For interpretation of the references to color in this figure legend, the reader is referred to the Web version of this article.)

support the growth of thick biofilms. In the case of the oxt10 mutant, growing the bioanodes with 1 mM, which supports the growth of biofilms ~20-μm thick [60], was sufficient to harvest current from acetate in the presence of oxygen.

Implications

The results presented herein demonstrate that *G. sulfurreducens* has natural mechanisms for antioxidant protection that can be harnessed to improve the performance of MECs with oxygen. The isolation of 11 oxt mutants with unique inactivating mutations yet similar oxygen-tolerant biofilm phenotypes is consistent with the presence of convergent pathways for antioxidant protection in *G. sulfurreducens*. This finding highlights the many molecular networks that could be exploited to engineer strains with improved performance in oxygenated BESs. Particularly important for BES applications is better understanding of the cellular mechanisms that allowed the oxt10 mutant to outperform the WT strain during the colonization of anode electrodes. The oxt10 mutation inactivated a DNA repair pathway (SbcCD nuclease) that may have triggered a chronic oxidative stress response in the cells. The aggregative behavior of this mutant, enhanced biofilm phenotype under oxic and anoxic conditions, and rapid attachment to the anode electrode are phenotypic indicators of the overproduction of an extracellular polymer such as a capsule. This polymeric barrier may have antioxidant and oxygen-extrusion activities, as reported for the EPS layers produced by other bacteria [2,67,71]. This very same mechanism could explain the growth advantage of this mutant during the reduction of Fe(III) oxides and its inability to grow with oxygen as sole electron acceptor. Future studies should, therefore, focus on the molecular and biochemical characterization of the oxt10 surface chemistry. This information could inform strategies to engineer electricigens with protective polymeric layers that reduce MEC start-up and prevent power drops during oxygen intrusions.

Also important for MEC applications is improved molecular understanding of how electroactive biofilms increase their oxidative stress response as they grow on the anode electrode. *G. sulfurreducens* regulates the growth and electroactivity of anode biofilms in MECs to optimize electron transport via matrix-associated cytochromes and conductive pili [60]. Less well known is the fact that these biofilms undergo a phase of maturation upon reaching their maximum height that increases the electroactivity and chemical resistance of the surface-attached communities [15]. This process is analogous to the activation of protective mechanisms against antimicrobials, heavy metals and other chemical stressors during the growth and maturation of other bacterial biofilms [29,42]. Yet, electroactive biofilms growing on anode electrodes activate mechanisms for antioxidant protection, a phenotypic trait that could be exploited via genetic engineering to minimize the negative impact of oxygen intrusions in MECs. The fact that thick biofilms have enhanced oxygen tolerance in MECs also affords opportunities for operational control of bioanode growth. Acetate is the preferred electron donor and carbon source for *Geobacter* electricigens [48] and its availability controls the growth of the biofilm cells on the anode electrode [60]. However, other combinations of electron donors can be used to promote the growth of robust bioanodes and minimize power losses to oxygen. For example, it is also possible to grow thick electroactive biofilms and reach high power densities with formate as long as small amounts of acetate are provided to facilitate the assimilation of formate carbon [57]. Like formate, higher voltages are predicted for lactate than acetate [33], yet metabolic constraints during the oxidation of lactate limit the growth of *G. sulfurreducens* on the anode electrode and reduce MEC performance [57]. However, strains adaptively evolved to overcome the metabolic bottlenecks grow thick bioanodes and sustain power densities with lactate as high as in acetate-fed MECs [5]. These lactate-improved strains can be co-inoculated in the anode chamber together with other engineered strains to form thick, hybrid bioanodes and improve the performance of MECs fed with mixes of electron donors [5]. Hence, strain improvement and MEC operation can be custom-tailored to grow robust bioanodes and address performance issues, as needed for specific applications.

Materials and methods

Bacterial strains and culture conditions

We routinely cultured the wild-type (WT) strain of *G. sulfurreducens* PCA at 30 °C in a mineral NB medium with 20 mM acetate and 40 mM fumarate (NBAF) supplemented with 1 mM cysteine and 0.1% yeast extract (NBAFYE), as described elsewhere [17]. Culturing of cells for microbial electrolysis cell (MEC) experiments used anaerobic DB medium [57] containing 20 mM acetate and 40 mM fumarate (DBAF) [57]. When indicated, we also grew the cells in a modified fresh water (FW) medium [13] supplemented with 20 mM acetate and 125 mM poorly crystalline Fe(III) oxides (FWAFeOx) with or without 1 mM of nitrilotriacetic acid (NTA), a chelator that stimulates growth with the Fe(III) oxides [59]. All media were sparged with N_2:CO_2 (80:20), sealed with butyl rubber stoppers, and autoclaved prior to use following standard anaerobic techniques [56]. Growth was routinely monitored spectrophotometrically at 600 nm (OD_{600}), except in the FWAFeOx cultures where increases in cell numbers were indirectly measured as HCl-extractable Fe(II) resulting from the reduction of Fe(III), as previously described [40].

Transposon mutagenesis and oxygen-tolerance screening

We constructed a library of Tn*5* mutants by mixing 100 μl of chilled

electrocompetent cells of *G. sulfurreducens* (prepared as described elsewhere [17]) with 1 μl of a kanamycin-resistant EZ-TN5 transposome (a Tn*5* transposon in synaptic complex with the Tnp transposon, from EpiCentre). After electroporation at 1.47 kV for 3.8 s, we gently mixed the electroporation solution with 1 ml of phosphate-buffered NBAF medium [17] and transferred the mix to a pre-reduced tube of NBAFYE medium previously warmed at 30 °C. We then incubated the cell suspension (OD_{600} of 0.339) at 30 °C for post-electroporation recovery.

The screening to identify oxygen tolerant (oxt) mutants used anoxic soft-agar tubes prepared with NBAF medium containing 1 ml/L of 0.1% resazurin (redox indicator) and 3 g/L of Noble agar (Difco). We sparged the media in the tubes with an oxygen-free gas mix of N_2:CO_2 (80:20) for 30 min before sealing them with a butyl rubber stopper and aluminum crimps. Once sterilized by autoclaving for 20 min, we cooled down the tubes in a 50 °C water bath and added kanamycin (50 μg/ml). We then inoculated each 10-ml tube of liquified soft agar with 0.2 ml of the Tn*5* library growing in the electroporation recovery tube (OD_{600}~0.5), mixed by inversion and incubated at 30 °C for 72 h. This method produced 20 soft-agar tubes to screen a full library of Tn*5* insertion mutants for oxygen tolerance.

After the initial anaerobic incubation of soft-agar tubes for 72 h, we replaced 30 ml of the tube's headspace with filter-sterilized air. The introduction of air in the tubes established a gradient of oxygen along the top ¾ region of the soft agar, which was visible as a pink coloration caused by the oxidation of resazurin. The ¼ bottom region of the tubes was colorless, thus substantially anoxic. We then incubated the soft-agar tubes at 30 °C for an additional 48 h until colonies were visible in the oxygenated zone. We used a syringe and a needle to retrieve 11 large colonies that grew in the upper region of the soft agar tubes (highest levels of oxygenation) and designated the clones as oxygen tolerant (oxt) mutant strains 1 to 11. We transferred each colony to an anoxic tube containing 10 ml of FWFA medium with kanamycin (50 μg/ml) and incubated at 30 °C to grow them into planktonic cultures. After three transfers in exponential phase, we prepared aliquots (1 ml culture mixed with 100 μl of DMSO) for cryopreservation at −80 °C.

Biofilm assays

We assayed the biofilm-forming abilities of the WT and oxt mutant biofilms under anoxic and oxic conditions in 48-well Corning® Costar® TC-Treated Multiple Well plates. Each strain was grown at 30 °C in 5 replicate wells containing FWFA medium. We incubated the anoxic cultures inside a gloved anaerobic chamber bag (COY Labs) containing an oxygen-free atmosphere of H_2:N_2:CO_2 (7:73:20) for 86 h. A replica set of plates was incubated under the same anoxic conditions for 30 h before transferring them to another incubator outside the glove bag to complete the incubation period (56 h) aerobically (anoxic=>oxic cultures). We also included control plates that were incubated aerobically for the full 86-h period (oxic cultures). As a negative control for the biofilm assay, we included in each plate 5 wells containing the medium but no cells (uninoculated control). At the end of the incubation period, we discarded the planktonic culture, stained the biofilms with 0.5 ml of 0.1% (w/v) crystal violet, solubilized the biofilm-associated dye with 0.5 ml of 33% acetic acid and measured the absorbance of the solution at 590 nm (A_{590}). We then subtracted the average A_{590} of the uninoculated control wells to calculate the biofilm biomass for each biological replicate. We identified statistically significant differences between the biofilm biomass of the oxt mutants and the WT with the two-tailed *t*-test analysis function in the Microsoft Excel software (*, $p < 0.05$; **, $p < 0.005$; ***, $p < 0.0005$).

Identification of transposon-insertion sites via rescue cloning

We used rescue cloning [35] to identify the site of transposon insertion in the genomes of the oxt mutants. We first purified genomic DNA from the oxt mutants using the MasterPure DNA Purification Kit (Epicentre Biotechnologies) and digested 1 μg of genomic DNA with the HindIII restriction enzyme (New England Biolabs) overnight. After self-ligation with T4 Ligase (Invitrogen), we transformed the plasmids into chemically competent *pir*+ cells of *Escherichia coli* and plated the transformants on Lysogeny Broth (LB) agar supplemented with 50 μg/ml of kanamycin. We then incubated the plates at 37 °C and grew individual colonies in LB cultures with kanamycin (50 μg/ml) before isolating the plasmid DNA with the Plasmid Mini Kit (Qiagen). Sanger sequencing of the Tn*5* flanking regions in the rescued replicative plasmid used the Tn*5* reverse sequencing primer (R6KAN-2-RP-1: 5′ CTACCCTGTGGAACACCTACATCT 3′) and standard protocols developed at the Genomics Core of the Research Technology and Support Facility (Michigan State University). The sequence of the region flanking the Tn5 insertion was identified using the Basic Local Alignment Search Tool (BLAST) available at the U.S. National Library of Medicine (NCBI). Protein identification and genome region analyses used the tools available at the Kyoto Encyclopedia of Genes and Genomes (KEGG).

Oxygen tolerance and reduction assays

We tested the ability of the WT and oxt (1-11) strains to tolerate and respire oxygen under microaerobic conditions with protocols modified from those described previously [37]. Notably, all incubations were at 35 °C, the optimal temperature for *G. sulfurreducens* growth. To test for oxygen tolerance, we grew the WT and oxt mutans to late exponential phase in anaerobic NBAFYE media buffered with 20 mM 3-(*N*-morpholino)propanesulfonic acid (MOPS) at pH 7.0 before transferring the cells to 50-ml serum bottles containing 25 ml of aerobic NBAFYE-MOPS medium (initial OD_{600} of 0.04). After 36 h of oxygen exposure, we transferred the cells (OD_{600} of 0.02) to triplicate tubes containing 10 ml of anaerobic NBAFYE-MOPS medium and monitored (OD_{600}) every ca. 6 h while incubating at 35 °C in the presence of oxygen. As anoxic controls, we also grew the strains anaerobically for 36 h in the 25-ml NBAFYE-MOPS bottles and transferred them to triplicate tubes of anoxic NBAFYE-MOPS medium.

To test for growth with oxygen as sole electron acceptor, we grew the WT and oxt mutant cells from an initial OD_{600} of 0.02 in triplicate tubes containing 10 ml of NBAFYE-MOPS prepared without cysteine and with a growth-limiting concentration of fumarate (20 mM instead of 40 mM). We monitored growth in the tubes spectrophotometrically until the cells depleted fumarate and stopped growing (entry in stationary phase at ~36 h). We then injected in the tube's headspace 8.5 ml of filter-sterilized air (the equivalent of 10% v/v of oxygen) and continued incubation at 35 °C for an additional 36 h while monitoring growth (OD_{600}) with oxygen as electron acceptor.

Microbial Electrolysis Cells (MECs)

We set up dual-chambered, H-type MECs inside a 30 °C incubator, as described previously [57]. The anode and cathode chambers contained 90 ml of DB medium containing acetate as the electron donor (typically 1 mM, but also 3 or 5 mM, as indicated) and a ~55 ml of headspace. We inserted in the anode chamber a reference electrode (previously sterilized in 70% ethanol for 1 min and rinsed with sterile water) and used it to poise the anode electrode to 0.24 V with a VSP potentiostat (Bio-Logic). We then sparged the anode and cathode chambers with filter-sterilized N_2:CO_2 (80:20) gas to make the media anoxic. Once the current stabilized, we inoculated the anode chamber with cells of *G. sulfurreducens* harvested from a stationary-phase DBAF cultures, as described previously [57]. The generation of an electrical current above the baseline marked the irreversible attachment of the cells to the anode electrode, while the linear phase of acceleration of the current signal matched the vertical growth of the attached cells into a multilayered, electroactive biofilm [58]. The deceleration phase in current production marked the end of biofilm growth due to the progressive depletion of acetate, which we measured periodically in culture supernatant fluids by

High Performance Liquid Chromatrography (Waters HPLC system, Milford, MA) at 30 °C, as previously described [57]. When indicated, we stopped gas sparging in the anode chamber and injected 20 ml (~169 μmoles of oxygen) or 10 ml (~85 μmoles of oxygen) of filter-sterilized air to investigate the response and recovery of current harvesting by the WT and oxt10 bioanodes to oxygen intrusions. Oxygen levels in the headspace of the anode chamber were analyzed periodically by gas chromatography (GC) using a Varian CP-4900 Micro Gas Chromatograph (Agilent, Santa Clara, CA). For post-exposure recovery experiments, we resumed the flow of the anoxic gas mix into the anode chamber (usually once the electrical current had reached baseline levels) and monitored the restart of current harvesting. When needed, we also supplemented the anode growth medium with acetate as electron donor to sustain current harvesting during the recovery phase.

Availability of data and materials

The strains described in this work are available upon request and conditioned to approval of material transfer agreements by Michigan State University.

CRediT authorship contribution statement

Allison M. Speers: conceived the study, interpreted the results and wrote the paper, performed all the experiments, The authors read and approved the final version of the manuscript. **Gemma Reguera:** and.

Declaration of competing interest

The authors declare that they have no known competing financial interests or personal relationships that could have appeared to influence the work reported in this paper.

Acknowledgements

The authors thank Dr. Dena Cologgi for assistance with the transposon mutagenesis and rescue cloning experiments and Kwi Kim for help with media preparation and HPLC analyses.

List of abbreviations

BES	Bioelectrochemical System
MEC	Microbial Electrolysis Cell
Oxt	Oxygen Tolerant
ROS	Reactive Oxygen Species
Tn5	Transposon 5
WT	Wild type

Ethics approval and consent to participate

Not applicable.

Consent for publication

Not applicable.

Funding

This work was supported by a Strategic Partnership grant from the Michigan State University Foundation, the Great Lakes Bioenergy Research Center (DOE BER Office of Science DE-FC02-07ER64494) and USDA National Institute of Food and Agriculture (Hatch project 1011745) to GR. We also acknowledge support from a Marvin Hensley Endowed, continuation, and dissertation completion fellowships from Michigan State's College of Natural Sciences to AMS.

References

[1] Adrian PV, Klugman KP. Mutations in the dihydrofolate reductase gene of trimethoprim-resistant isolates of *Streptococcus pneumoniae*. Antimicrob Agents Chemother 1997;41(11):2406–13. https://doi.org/10.1128/AAC.41.11.2406.
[2] Andrew M, Jayaraman G. Structural features of microbial exopolysaccharides in relation to their antioxidant activity. Carbohydr Res 2020;487:107881. https://doi.org/10.1016/j.carres.2019.107881.
[3] Anzaldi LL, Skaar EP. Overcoming the heme paradox: heme toxicity and tolerance in bacterial pathogens. Infect Immun 2010;78(12):4977–89. https://doi.org/10.1128/iai.00613-10.
[4] Atci E, Babauta JT, Sultana ST, Beyenal H. Microbiosensor for the detection of acetate in electrode-respiring biofilms. Biosens Bioelectron 2016;81:517–23. https://doi.org/10.1016/j.bios.2016.03.027.
[5] Awate B, Steidl RJ, Hamlischer T, Reguera G. Stimulation of electro-fermentation in single-chamber microbial electrolysis cells driven by genetically engineered anode biofilms. J Power Sources 2017;356:510–8. https://doi.org/10.1016/j.jpowsour.2017.02.053.
[6] Babauta JT, Beasley CA, Beyenal H. Investigation of electron transfer by *Geobacter sulfurreducens* biofilms by using an electrochemical quartz crystal microbalance. ChemElectroChem 2014;1(11):2007–16. https://doi.org/10.1002/celc.201402127.
[7] Babauta JT, Beyenal H. Mass transfer studies of *Geobacter sulfurreducens* biofilms on rotating disk electrodes. Biotechnol Bioeng 2014;111(2):285–94. https://doi.org/10.1002/bit.25105.
[8] Bharat A, Jiang M, Sullivan SM, Maddock JR, Brown ED. Cooperative and critical roles for both G domains in the GTPase activity and cellular function of ribosome-associated *Escherichia coli* EngA. J Bacteriol 2006;188(22):7992–6. https://doi.org/10.1128/JB.00959-06.
[9] Borole AP, Reguera G, Ringeisen B, Wang Z-W, Feng Y, Kim BH. Electroactive biofilms: current status and future research needs. Energy Environ Sci 2011;4:4813–34. https://doi.org/10.1039/C1EE02511B.
[10] Butler JE, Kaufmann F, Coppi MV, Nunez C, Lovley DR. MacA, a diheme *c*-type cytochrome involved in Fe(III) reduction by *Geobacter sulfurreducens*. J Bacteriol 2004;186(12):4042–5. https://doi.org/10.1128/JB.186.12.4042-4045.2004.
[11] Cardenas JP, Quatrini R, Holmes DS. Aerobic lineage of the oxidative stress response protein rubrerythrin emerged in an ancient microaerobic, (hyper) thermophilic environment. Front Microbiol 2016;7(1822). https://doi.org/10.3389/fmicb.2016.01822.
[12] Cheng S, Liu H, Logan BE. Increased power generation in a continuous flow MFC with advective flow through the porous anode and reduced electrode spacing. Environ Sci Technol 2006;40(7):2426–32. https://doi.org/10.1021/es051652w.
[13] Cologgi DL, Lampa-Pastirk S, Speers AM, Kelly SD, Reguera G. Extracellular reduction of uranium via *Geobacter* conductive pili as a protective cellular mechanism. Proc Natl Acad Sci USA 2011;108(37):15248–52. https://doi.org/10.1073/pnas.1108616108.
[14] Cologgi DL, Otwell AE, Speers AM, Rotondo J, Reguera G. Genetic analysis of electroactive biofilms. Int Microbiol 2021. https://doi.org/10.1007/s10123-021-00176-y.
[15] Cologgi DL, Speers AM, Bullard BA, Kelly SD, Reguera G. Enhanced uranium immobilization and reduction by *Geobacter sulfurreducens* biofilms. Appl Environ Microbiol 2014;80(21):6638–46. https://doi.org/10.1128/AEM.02289-14.
[16] Connelly JC, Kirkham LA, Leach DRF. The SbcCD nuclease of *Escherichia coli* is a structural maintenance of chromosomes (SMC) family protein that cleaves hairpin DNA. Proc Nat Acad Sci USA 1998;95(14):7969–74. https://doi.org/10.1073/pnas.95.14.7969.
[17] Coppi MV, Leang C, Sandler SJ, Lovley DR. Development of a genetic system for *Geobacter sulfurreducens*. Appl Environ Microbiol 2001;67(7):3180–7. https://doi.org/10.1128/AEM.67.7.3180-3187.2001.
[18] Coulon J, Matoub L, Dossot M, Marchand S, Bartosz G, Leroy P. Potential relationship between glutathione metabolism and flocculation in the yeast *Kluyveromyces lactis*. FEMS Yeast Res 2007;7(1):93–101. https://doi.org/10.1111/j.1567-1364.2006.00146.x.
[19] Dailey HA, Dailey TA, Gerdes S, Jahn D, Jahn M, Brian MR, Warren MJ. Prokaryotic heme biosynthesis: Multiple pathways to a common essential product. Microbiol Mol Biol Rev 2017;81(1):e00048. https://doi.org/10.1128/MMBR.00048-16. 00016.
[20] Darie S, Gunsalus RP. Effect of heme and oxygen availability on *hemA* gene expression in *Escherichia coli*: role of the *fnr, arcA*, and *himA* gene products. J Bacteriol 1994;176(17):5270–6. https://doi.org/10.1128/jb.176.17.5270-5276.1994.
[21] Dulay H, Tabares M, Kashefi K, Reguera G. Cobalt resistance via detoxification and mineralization in the iron-reducing bacterium *Geobacter sulfurreducens*. Front Microbiol 2020;11(2992):600463. https://doi.org/10.3389/fmicb.2020.600463.
[22] Engel CEA, Vorländer D, Biedendieck R, Krull R, Dohnt K. Quantification of microaerobic growth of *Geobacter sulfurreducens*. PloS One 2020;15(1):e0215341. https://doi.org/10.1371/journal.pone.0215341.
[23] Ercal N, Gurer-Orhan H, Aykin-Burns N. Toxic metals and oxidative stress part I: mechanisms involved in metal-induced oxidative damage. Curr Top Med Chem 2001;1(6):529–39. https://doi.org/10.2174/1568026013394831.
[24] Ezraty B, Gennaris A, Barras F, Collet J-F. Oxidative stress, protein damage and repair in bacteria. Nat Rev Microbiol 2017;15(7):385–96. https://doi.org/10.1038/nrmicro.2017.26.
[25] Gaharwar US, Meena R, Rajamani P. Iron oxide nanoparticles induced cytotoxicity, oxidative stress and DNA damage in lymphocytes. J Appl Toxicol 2017;37(10):1232–44. https://doi.org/10.1002/jat.3485.

[26] Galaris D, Barbouti A, Pantopoulos K. Iron homeostasis and oxidative stress: an intimate relationship. Biochim Biophys Acta Mol Cell Res 2019;1866(12):118535. https://doi.org/10.1016/j.bbamcr.2019.118535.

[27] Gambino M, Cappitelli F. Mini-review: biofilm responses to oxidative stress. Biofouling 2016;32(2):167–78. https://doi.org/10.1080/08927014.2015.1134515.

[28] Harms K, Wackernagel W. The RecBCD and SbcCD DNases suppress homology-facilitated illegitimate recombination during natural transformation of *Acinetobacter baylyi*. Microbiology 2008;154(8):2437–45. https://doi.org/10.1099/mic.0.2008/018382-0.

[29] Harrison JJ, Ceri H, Turner RJ. Multimetal resistance and tolerance in microbial biofilms. Nat Rev Microbiol 2007;5(12):928–38. https://doi.org/10.1038/nrmicro1774.

[30] Imlay JA. Pathways of oxidative damage. Annu Rev Microbiol 2003;57:395–418. https://doi.org/10.1146/annurev.micro.57.030502.090938.

[31] Imlay JA. Cellular defenses against superoxide and hydrogen peroxide. Annu Rev Biochem 2008;77:755–76. https://doi.org/10.1146/annurev.biochem.77.061606.161055.

[32] Jog R, Chen G, Wang J, Leff T. A potential link between glycine metabolism, glutathione and diabetes. Faseb J 2019;33(S1):590. https://doi.org/10.1096/fasebj.2019.33.1_supplement.590.3. 593-590.593.

[33] Kiely PD, Call DF, Yates MD, Regan JM, Logan BE. Anodic biofilms in microbial fuel cells harbor low numbers of higher-power-producing bacteria than abundant genera. Appl Microbiol Biotechnol 2010;88(1):371–80. https://doi.org/10.1007/s00253-010-2757-2.

[34] Kim JR, Cheng S, Oh S-E, Logan BE. Power generation using different cation, anion, and ultrafiltration membranes in microbial fuel cells. Environ Sci Technol 2007;41(3):1004–9. https://doi.org/10.1021/es062202m.

[35] Kirby JR. In vivo mutagenesis using EZ-*Tn5*. Methods Enzymol 2007;421:17–21. https://doi.org/10.1016/S0076-6879(06)21003-6.

[36] Lampa-Pastirk S, Veazey JP, Walsh KA, Feliciano GT, Steidl RJ, Tessmer SH, Reguera G. Thermally activated charge transport in microbial protein nanowires. Sci Rep 2016;6:23517. https://doi.org/10.1038/srep23517.

[37] Lin WC, Coppi MV, Lovley DR. *Geobacter sulfurreducens* can grow with oxygen as a terminal electron acceptor. Appl Environ Microbiol 2004;70(4):2525–8. 70.4.2525-2528.2004.

[38] Liu CT, Hanoian P, French JB, Pringle TH, Hammes-Schiffer S, Benkovic SJ. Functional significance of evolving protein sequence in dihydrofolate reductase from bacteria to humans. Proc Nat Acad Sci USA 2013;110(25):10159–64. https://doi.org/10.1073/pnas.1307130110.

[39] Liu X, Sun X, Wu Y, Xie C, Zhang W, Wang D, Chen X, Qu D, Gan J, Chen H, Jiang H, Lan L, Yang C-G. Oxidation-sensing regulator AbfR regulates oxidative stress responses, bacterial aggregation, and biofilm formation in *Staphylococcus epidermidis*. J Biol Chem 2013;288(6):3739–52. https://doi.org/10.1074/jbc.M112.426205.

[40] Lovley DR, Phillips EJ. Rapid assay for microbially reducible ferric iron in aquatic sediments. Appl Environ Microbiol 1987;53(7):1536–40.

[41] Lubelski J, Konings WN, Driessen AJM. Distribution and physiology of ABC-type transporters contributing to multidrug resistance in bacteria. Microbiol Mol Biol Rev 2007;71(3):463–76. https://doi.org/10.1128/MMBR.00001-07.

[42] Mah TF, Pitts B, Pellock B, Walker GC, Stewart PS, O'Toole GA. A genetic basis for *Pseudomonas aeruginosa* biofilm antibiotic resistance. Nature 2003;426(6964):306–10. https://doi.org/10.1038/nature02122.

[43] Mikkelsen H, Duck Z, Lilley KS, Welch M. Interrelationships between colonies, biofilms, and planktonic cells of *Pseudomonas aeruginosa*. J Bacteriol 2007;189(6):2411–6. https://doi.org/10.1128/JB.01687-06.

[44] Moya A, Guimerà X, del Campo FJ, Prats-Alfonso E, Dorado AD, Baeza M, Villa R, Gabriel D, Gamisans X, Gabriel G. Biofilm oxygen profiling using an array of microelectrodes on a microfabricated needle. Procedia Eng 2014;87:256–9. https://doi.org/10.1016/j.proeng.2014.11.654.

[45] Oh SE, Kim JR, Joo J-H, Logan BE. Effects of applied voltages and dissolved oxygen on sustained power generation by microbial fuel cells. Water Sci Technol 2009;60(5):1311–7. https://doi.org/10.2166/wst.2009.444.

[46] Pereira MC, Oliveira LCA, Murad E. Iron oxide catalysts: Fenton and Fenton-like reactions – a review. Clay Miner 2012;47(3):285–302. https://doi.org/10.1180/claymin.2012.047.3.01.

[47] Poole K. Bacterial stress responses as determinants of antimicrobial resistance. J Antimicrob Chemother 2012;67(9):2069–89. https://doi.org/10.1093/jac/dks196.

[48] Reguera G, Kashefi K. The electrifying physiology of *Geobacter* bacteria, 30 years on. Adv Microb Physiol 2019;74:1–96. https://doi.org/10.1016/bs.ampbs.2019.02.007.

[49] Reguera G, McCarthy KD, Mehta T, Nicoll JS, Tuominen MT, Lovley DR. Extracellular electron transfer via microbial nanowires. Nature 2005;435(7045):1098–101. https://doi.org/10.1038/nature03661.

[50] Reguera G, Nevin KP, Nicoll JS, Covalla SF, Woodard TL, Lovley DR. Biofilm and nanowire production lead to increased current in microbial fuel cells. Appl Environ Microbiol 2006;72(11):7345–8. https://doi.org/10.1128/AEM.01444-06.

[51] Reguera G, Pollina RB, Nicoll JS, Lovley DR. Possible nonconductive role of *Geobacter sulfurreducens* pilus nanowires in biofilm formation. J Bacteriol 2007;189(5):2125–7. https://doi.org/10.1128/JB.01284-06.

[52] Seidel J, Hoffmann M, Ellis KE, Seidel A, Spatzal T, Gerhardt S, Elliott SJ, Einsle O. MacA is a second cytochrome *c* peroxidase of *Geobacter sulfurreducens*. Biochemistry 2012;51(13):2747–56. https://doi.org/10.1021/bi300249u.

[53] Shioi J, Dang CV, Taylor BL. Oxygen as attractant and repellent in bacterial chemotaxis. J Bacteriol 1987;169(7):3118–23. https://doi.org/10.1128/jb.169.7.3118-3123.1987.

[54] Si M, Zhao C, Burkinshaw B, Zhang B, Wei D, Wang Y, Dong TG, Shen X. Manganese scavenging and oxidative stress response mediated by type VI secretion system in *Burkholderia thailandensis*. Proc Natl Acad Sci USA 2017;114(11):E2233–e2242. https://doi.org/10.1073/pnas.1614902114.

[55] Slade D, Radman M. Oxidative stress resistance in *Deinococcus radiodurans*. Microbiol Mol Biol Rev 2011;75(1):133–91. https://doi.org/10.1128/MMBR.00015-10.

[56] Speers AM, Cologgi DL, Reguera G. Anaerobic cell culture. Curr Protocols Microbiol Appendix 2009;4. https://doi.org/10.1002/9780471729259.mca04fs12. Appendix 4F.

[57] Speers AM, Reguera G. Electron donors supporting growth and electroactivity of *Geobacter sulfurreducens* anode biofilms. Appl Environ Microbiol 2012;78(2):437–44. https://doi.org/10.1128/aem.06782-11.

[58] Speers AM, Reguera G. Theoretical and practical considerations for culturing *Geobacter* biofilms in microbial fuel cells and other bioelectrochemical systems. In: Beyenal H, Babauta J, editors. Biofilms in bioelectrochemical systems. John Wiley & Sons, Inc; 2015. p. 37–60. https://doi.org/10.1002/9781119097426.ch2.

[59] Speers AM, Schindler BD, Hwang J, Genc A, Reguera G. Genetic identification of a PilT motor in *Geobacter sulfurreducens* reveals a role for pilus retraction in extracellular electron transfer. Front Microbiol 2016;7:1578. https://doi.org/10.3389/fmicb.2016.01578.

[60] Steidl R, Lampa-Pastirk S, Reguera G. Mechanistic stratification in electroactive biofilms of *Geobacter sulfurreducens* mediated by pilus nanowires. Nat Commun 2016;7:12217. https://doi.org/10.1038/ncomms12217.

[61] Stewart PS. Diffusion in biofilms. J Bacteriol 2003;185(5):1485–91.

[62] Storvik KA, Foster PL. The SMC-like protein complex SbcCD enhances DNA polymerase IV-dependent spontaneous mutation in *Escherichia coli*. J Bacteriol 2011;193(3):660–9. https://doi.org/10.1128/JB.01166-10.

[63] TerAvest MA, Rosenbaum MA, Kotloski NJ, Gralnick JA, Angenent LT. Oxygen allows *Shewanella oneidensis* MR-1 to overcome mediator washout in a continuously fed bioelectrochemical system. Biotechnol Bioeng 2014;111(4):692–9. https://doi.org/10.1002/bit.25128.

[64] Thorpe GW, Fong CS, Alic N, Higgins VJ, Dawes IW. Cells have distinct mechanisms to maintain protection against different reactive oxygen species: oxidative-stress-response genes. Proc Natl Acad Sci USA 2004;101(17):6564–9. https://doi.org/10.1073/pnas.0305888101.

[65] Van Houten B, Santa-Gonzalez GA, Camargo M. DNA repair after oxidative stress: current challenges. Curr Opin Toxicol 2018;7:9–16. https://doi.org/10.1016/j.cotox.2017.10.009.

[66] Wang W, Wu Z, Lin G, Hu S, Wang B, Dai Z, Wu G. Glycine stimulates protein synthesis and inhibits oxidative stress in pig small intestinal epithelial cells. J Nutr 2014;144(10):1540–8. https://doi.org/10.3945/jn.114.194001.

[67] Yan M, Wang BH, Xu X, der Meister Jr T, Tabyac HT, Hwang FF, Liu Z. Extrusion of dissolved oxygen by exopolysaccharide from *Leuconostoc mesenteroides* and its Implications in relief of the oxygen stress. Front Microbiol 2018;9:2467. https://doi.org/10.3389/fmicb.2018.02467.

[68] Yang J, Cheng S, Li P, Huang H, Cen K. Sensitivity to oxygen in microbial electrochemical systems biofilms. iScience 2019;13:163–72. https://doi.org/10.1016/j.isci.2019.01.022.

[69] Zahradka K, Buljubašić M, Petranović M, Zahradka D. Roles of ExoI and SbcCD nucleases in "reckless" DNA degradation in *recA* mutants of *Escherichia coli*. J Bacteriol 2009;191(5):1677–87. https://doi.org/10.1128/jb.01877-07.

[70] Zeman MK, Cimprich KA. Causes and consequences of replication stress. Nat Cell Biol 2014;16(1):2–9. https://doi.org/10.1038/ncb2897.

[71] Zhang L, Liu C, Li D, Zhao Y, Zhang X, Zeng X, Yang Z, Li S. Antioxidant activity of an exopolysaccharide isolated from *Lactobacillus plantarum* C88. Int J Biol Macromol 2013;54:270–5. https://doi.org/10.1016/j.ijbiomac.2012.12.037.